Neuron
Article

Slit2 Activity in the Migration of Guidepost Neurons Shapes Thalamic Projections during Development and Evolution

Franck Bielle,[1,2,3] Paula Marcos-Mondejar,[4,9] Maryama Keita,[1,2,3,9] Caroline Mailhes,[1,2,3] Catherine Verney,[5,6] Kim Nguyen Ba-Charvet,[7] Marc Tessier-Lavigne,[8] Guillermina Lopez-Bendito,[4] and Sonia Garel[1,2,3,*]
[1]Inserm, U1024, 75005 Paris, France
[2]CNRS, UMR 8197, 75005 Paris, France
[3]Ecole Normale Supérieure, Institut de Biologie de l'ENS, IBENS, 46 rue d'Ulm, 75005 Paris, France
[4]Instituto de Neurociencias de Alicante, Universidad Miguel Hernandez-Consejo Superior de Investigaciones Científicas (UMH-CSIC), San Joan d'Alacant 03550, Spain
[5]Université Paris Diderot-Paris 7, 75013 Paris, France
[6]Inserm, U676, Hôpital Robert Debré, 75019 Paris, France
[7]Inserm, U592, Institut de la vision, 75012 Paris, France
[8]Genentech, Inc., South San Francisco, CA 94080, USA
[9]These authors contributed equally to this work
*Correspondence: garel@biologie.ens.fr
DOI 10.1016/j.neuron.2011.02.026

SUMMARY

How brain connectivity has evolved to integrate the mammalian-specific neocortex remains largely unknown. Here, we address how dorsal thalamic axons, which constitute the main input to the neocortex, are directed internally to their evolutionary novel target in mammals, though they follow an external path to other targets in reptiles and birds. Using comparative studies and functional experiments in chick, we show that local species-specific differences in the migration of previously identified "corridor" guidepost neurons control the opening of a mammalian thalamocortical route. Using in vivo and ex vivo experiments in mice, we further demonstrate that the midline repellent Slit2 orients migration of corridor neurons and thereby switches thalamic axons from an external to a mammalian-specific internal path. Our study reveals that subtle differences in the migration of conserved intermediate target neurons trigger large-scale changes in thalamic connectivity, and opens perspectives on Slit functions and the evolution of brain wiring.

INTRODUCTION

Brain functioning relies on the formation of long-range axonal projections that follow a stereotyped pattern highly conserved among individuals of the same species. In mammals, the neocortex plays a fundamental role in major brain functions, including sensory perception, motor behavior, and cognition. It receives sensory input via a large thalamic projection highway that runs along an internal route through the forebrain called the internal capsule. Although the neocortex and its specific thalamocortical afference are unique to mammals, thalamic projections relay sensory information to other forebrain structures in all tetrapods (Butler, 1994). Therefore, in contrast to a large number of brain axonal tracts, thalamic projections show major differences among vertebrates: for instance, thalamic axons (TAs) mainly target ventral regions of the telencephalon through an external path in reptiles and birds (Butler, 1994; Cordery and Molnar, 1999; Redies et al., 1997). What controls the differential pathfinding of TAs in mammals versus nonmammalian vertebrates and how these essential projections have evolved remain unknown.

Studies in rodents have led to the characterization of cellular and molecular actors that participate in the guidance of pioneer thalamocortical axons toward the neocortex. Thalamocortical axons start to form during early embryogenesis and follow a complex pathway: they run through the ventral thalamus, travel internally through the ventral telencephalon—through the medial ganglionic eminence (MGE) and the lateral ganglionic eminence (LGE)—and reach the neocortex (Auladell et al., 2000; Lopez-Bendito and Molnar, 2003; Metin and Godement, 1996; Molnar et al., 1998). Several studies have revealed that the ventral telencephalon is a major intermediate target for these axons (Braisted et al., 1999; Metin and Godement, 1996; Molnar et al., 1998). For instance, guidepost neurons forming early projections to the dorsal thalamus have been proposed to promote the entrance of TAs into the ventral telencephalon (Metin and Godement, 1996; Mitrofanis and Baker, 1993; Molnar et al., 1998), and the local expression of protocadherins controls the further progression of thalamocortical connections (Uemura et al., 2007; Zhou et al., 2008). Finally, several classical guidance cues have been shown to control specific steps of TA navigation along their path toward the neocortex, including Netrin1, Neuregulin1 (Nrg1), and Slit2 (Bagri et al., 2002; Braisted et al., 2000, 2009; Garel and Rubenstein, 2004; Leighton et al., 2001; Lin et al., 2003; Lopez-Bendito et al., 2006).

The secreted Slit proteins control a large number of cellular processes, including cell migration and axon guidance, via their

binding to Roundabout (Robo) receptors (Geisen et al., 2008; Nguyen-Ba-Charvet et al., 2004; Wu et al., 1999; Zhu et al., 1999). In particular, Slits and Robos control evolutionarily conserved guidance decisions during ventral midline crossing and positioning of longitudinal tracts, mainly via a repulsive activity (Brose et al., 1999; Farmer et al., 2008; Kidd et al., 1998; Long et al., 2004; Nguyen Ba-Charvet et al., 1999, 2002; Plump et al., 2002; Rajagopalan et al., 2000; Shu et al., 2003b; Simpson et al., 2000). In the rodent forebrain, Slit2, Robo1, and Robo2 have been implicated in the guidance of several major axonal tracts, including TAs (Andrews et al., 2006; Bagri et al., 2002; Braisted et al., 2009; Lopez-Bendito et al., 2007). For instance, Slit2, and to a lesser extent Slit1, mediates a repulsive activity that prevents axons from growing toward the ventral midline, by direct binding to Robo1 and Robo2 receptors (Bagri et al., 2002; Braisted et al., 2009; Lopez-Bendito et al., 2007).

In addition to the aforementioned guidance cues, we have shown in mice that a tangential neuronal cell migration from the LGE into the MGE is required to form a permissive corridor for pioneer TAs (Lopez-Bendito et al., 2006). These "corridor cells" follow an internal route within the nonpermissive MGE, and delineate the future path of growing TAs, by having a short-range activity via the expression of membrane-bound Nrg1 (Lopez-Bendito et al., 2006). However, the mechanisms underlying the positioning of corridor cells, which is essential for their short-range guidepost activity, are poorly understood (Simpson et al., 2009). In addition, how corridor neurons have acquired their internal guidepost function during evolution remains to be elucidated.

Here, we address how TA pathfinding is differentially guided in mammal and reptile/bird embryos along an internal or external path, respectively. We found that species-specific TA trajectories diverge as they cross the MGE even though essential internal corridor neurons are conserved in mouse, human, sheep, turtle, snake, and chicken embryos. Combination of grafts in chicken and mouse embryos shows that a cardinal difference between mammals and birds lies in the local positioning of corridor neurons that have otherwise remarkably conserved axonal guidance properties. At the molecular level, the secreted factor Slit2 is differently expressed in the ventral telencephalon of the two species and acts as a short-range repellent on the migration of corridor cells. Using a combination of in vivo and ex vivo experiments in mice, we demonstrate that Slit2 is required to locally orient the migration of mammalian corridor cells and thereby switches the path of TAs from a default external route into an internal path to the neocortex. Taken together, our results show that the minor differences in the positioning of conserved neurons, which is controlled by Slit2, play an essential role in the species-specific pathfinding of TAs, thereby providing a framework to understand the shaping and evolution of a major forebrain projection.

RESULTS

The MGE Is a Decision Point for the Internal/External Path of TAs

TAs reach the mammalian neocortex via the internal capsule, whereas they join an external lateral forebrain bundle toward other structures in nonmammalian vertebrates (Butler, 1994; Cordery and Molnar, 1999; Redies et al., 1997). To understand how this major change in brain connectivity occurred, we first reexamined in detail the positioning of TAs in the ventral telencephalon of different species. We observed that already within the MGE mantle, TAs navigate internally in mammals, whereas they grow externally in reptiles/birds (Cordery and Molnar, 1999; Redies et al., 1997; Verney et al., 2001), as observed in mouse and chick embryos (Figure 1; data not shown). This difference can be further visualized by a comparison with early midbrain dopaminergic projections: whereas TAs and dopaminergic axons both navigate externally to the MGE mantle of reptiles/birds, they grow at distinct internal and external levels, respectively, in mammals (Cordery and Molnar, 1999; Redies et al., 1997; Verney et al., 2001) (Figures 1C, 1D, 1G, and 1H). Thus, TAs undertake different internal/external trajectories in the MGE, thereby supporting a role for this intermediate target.

Internal Corridor-like Cells Are Present in Mammalian, Reptile, and Avian Embryos

We previously showed that TA pathfinding in the mouse MGE is controlled by short-range guidepost corridor cells (Lopez-Bendito et al., 2006). Thus, we wondered if species-specific differences in corridor cells might participate in the selective internal/external trajectory of TAs. To explore this issue we examined if homologous corridor-like cells exist in several mammalian (sheep, human) and reptile/bird species (Chinese soft-shelled turtle, Nagashima et al., 2009; corn-snake, Gomez et al., 2008; and chicken) because it was described that corridor-like cells are not present in amphibians (Moreno and González, 2007; Moreno et al., 2008). We first defined a molecular fingerprint of mouse corridor cells: they form a continuum expanding from the striatum into the Nkx2.1-positive MGE, and they express Islet1 but express neither Nkx2.1 (Lopez-Bendito et al., 2006) nor Foxp2 (Figure 2A; data not shown). Using this molecular fingerprint, we showed that corridor-like cells are present in all the species we examined (Figure 2; data not shown). However, the shape of the corridor varied: in mammalian species the corridor expands "around" the GP (Figures 2A–2D), whereas it shows an expansion directed toward the midline in reptile/bird embryos (Figures 2E–2H). Taken together, our data show that, like most telencephalic tangential streams of cell migration (Cobos et al., 2001; Metin et al., 2007; Tuorto et al., 2003), corridor-like cells are evolutionary conserved in reptiles/birds.

Chicken Corridor-like Cells Are Permissive for the Growth of TAs

The observation that corridor-like cells exist in species with external TAs raised the possibility that the guidance properties of these cells may have been acquired in mammals. To examine the cellular properties of nonmammalian corridor cells, we took advantage of the chicken embryo, which provides a model accessible to experimental manipulations.

Because mouse corridor cells are LGE-derived neurons migrating tangentially into the MGE that express Islet1, *Ebf1*, *Meis2*, and *Nrg1* (Lopez-Bendito et al., 2006), we used these

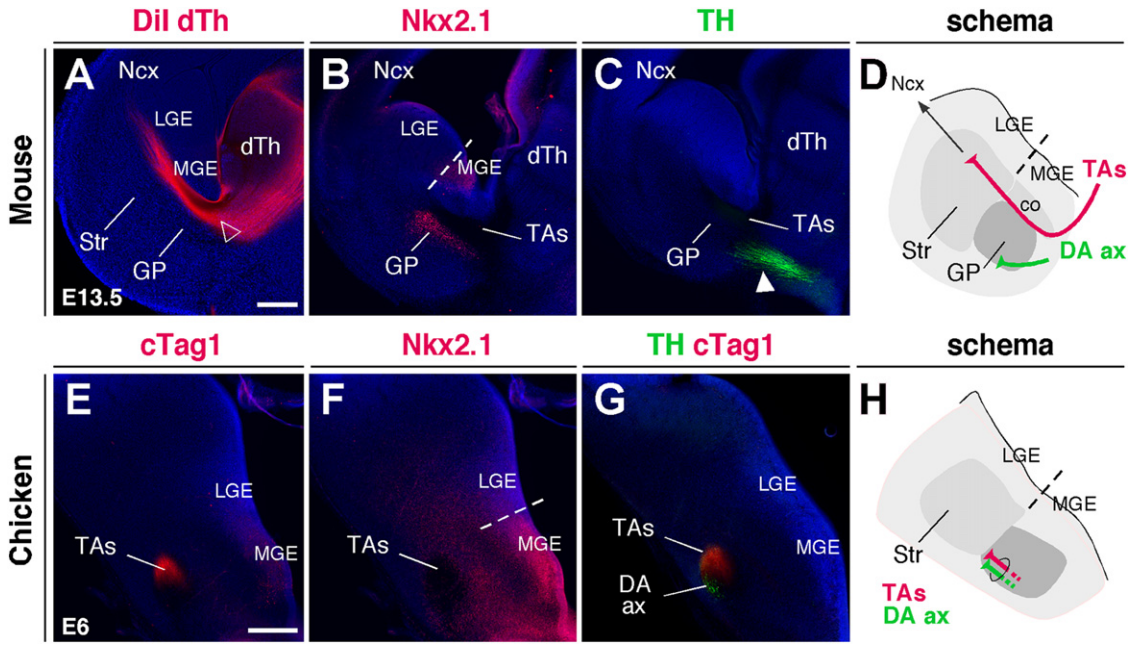

Figure 1. TA Paths in Mouse and Chicken Embryos Diverge in the MGE

(A–C) Forty-five degree angle sections (45° between coronal and sagittal planes) of E13.5 mouse embryos showing: (A) DiI tracing of TAs (open arrowhead); (B) Nkx2.1-positive GP; and (C) tyrosine hydroxylase (TH)-positive axons (solid arrowhead). Note that whereas TAs navigate in the corridor deep to the GP, TH-positive axons including dopaminergic axons grow through the superficial GP.

(D) Schematic representation of the internal path of TAs in mouse embryos.

(E–G) Coronal sections of E6 chicken embryos show the relative positioning of TAs, the MGE mantle, and TH-positive axons, labeled by immunohistochemistry against cTag1 (E), Nkx2.1 (F), and TH (G), respectively. Note that both TAs and dopaminergic projections navigate in the superficial part of the MGE.

(H) Schematic representation of the external path of TAs in chicken embryos.

ax, axons; co, corridor; DA, dopaminergic; dTh, dorsal thalamus; Ncx, neocortex; Str, striatum. Scale bars, 300 μm.

characteristics to examine chicken corridor-like cells. By performing DiI labeling in slice cultures and expression studies, we showed that corridor-like cells migrate tangentially from the LGE (n = 13/18) and express *cEbf1*, *cMeis2*, and *cNrg1*, thereby indicating that they share cellular and molecular properties with their mouse homologs (see Figure S1 available online; data not shown).

Although chicken corridor-like cells do not guide TAs in vivo, they express *cNrg1* (data not shown), suggesting the intriguing possibility that they might nevertheless exhibit permissive properties for TA growth. The guidepost activity of corridor cells in mice relies on the fact that these cells are permissive for TA growth and that TAs can respond to corridor-derived permissive cues. To test whether these properties are conserved in birds, we first grafted chicken dorsal thalamus explants into wild-type mouse embryonic brain slices in contact with the corridor (Figures 3A and 3B). Remarkably, we observed that chicken TAs grow in the mouse ventral telencephalon (n = 6/11; Figures 3A and 3B). Furthermore, these axons systematically navigate through the mouse corridor (n = 6/6) as well as in some cases along a superficial route (n = 3/6; Figures 3A and 3B), similar to what was described for mouse TAs (Lopez-Bendito et al., 2006). Thus, chicken TAs possess the cellular and molecular properties needed to be guided by mouse corridor cells. To further analyze the properties of chicken axons and corridor-like cells, we performed slice culture experiments in chicken in which we confronted dorsal thalamus explants to the MGE mantle (Figures 3C–3F). Using the corridor-like marker Islet1, we detected two strikingly different behaviors of TAs: when thalamic explants were not in contact with corridor-like cells, axons grew externally as in vivo (n = 7/7; Figures 3C and 3D), whereas they also navigate internally through corridor-like cells when explants were in contact (n = 12/13; Figures 3E and 3F). Therefore, when chicken corridor-like cells are in contact with TAs, they are sufficient to promote an internal growth of axons, similar to what is observed in mouse embryos.

A Distinct Corridor Shape in Chick Precludes an Interaction with TAs

The paradoxical observation that chicken corridor-like cells can guide TAs but do not act as guidepost cells in vivo prompted us to compare the relative positioning of corridor cells and ingrowing TAs in mouse and chicken embryos. To this aim, we performed in toto experiments on whole telencephalic vesicles (Figure 4). Using *Ebf1* as a marker of LGE mantle and corridor cells and *Dlx1* to label the entire ventral telencephalon (Lopez-Bendito et al., 2006), we observed that the mouse corridor has a fan shape that converges toward the caudomedial "corner" of the ventral telencephalon, before TA arrival (Figures 4A–4D; data not shown). Further labeling of TAs using the lipophilic tracer DiI shows that TAs enter the corridor by its caudal tip, indicating that this caudal part of the corridor is important for its guidepost

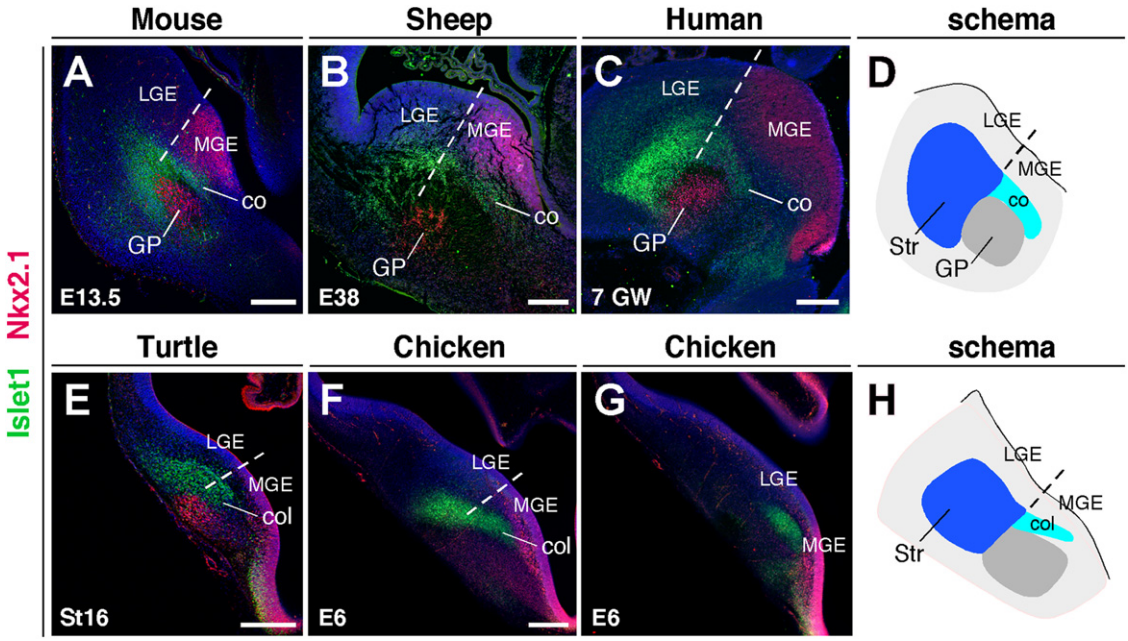

Figure 2. Corridor-like Cells Are Present in Mammalian, Reptile, and Avian Embryos

Islet1-positive Nkx2.1-negative corridor cells are detected in the MGE of coronal sections from E13.5 mouse embryo (A), E38 sheep embryo (B), 7 gestational weeks' human embryo (C), stage 16 Chinese soft-shelled turtle embryo (E), and E6 chicken embryo (intermediate level in F; caudal level in G). Schematic drawings of the corridor in mammalian and nonmammalian embryos are respectively presented in (D) and (H). Dotted lines mark the LGE/MGE boundary. co, corridor; col, corridor-like; GW, gestational weeks; Str, striatum. Scale bars, 300 μm.

activity (Figures 4E and 4F). In contrast, the *cEbf1*-positive chicken corridor converges medially and does not extend up to the caudal border of the ventral telencephalon, as visualized by *cDlx1* expression (Figures 4H–4K). This distant positioning of chicken corridor-like cells does not allow any potential interactions with TAs when they enter the ventral telencephalon (Figures 4L and 4M). Thus, corridor cells of the two species present a different three-dimensional organization that either allows or precludes an interaction with TAs (Figures 4G and 4N).

Overall, our experiments show that corridor-like cells with remarkably conserved guidance properties exist in an evolutionarily divergent species. However, their position in the ventral telencephalon prevents them from acting as guideposts for TAs that grow externally. These results reveal that the orientation of corridor cell migration constitutes an instrumental step in the opening of an internal pathfinding of TAs in the mammalian brain.

Slit2 Is a Candidate Factor to Orient the Species-Specific Shaping of the Corridor

To investigate the molecular mechanism underlying this process, we searched for molecular cues that may act differentially on corridor cell migration in mouse and chicken embryos.

To this aim, we first examined the cellular activities controlling the positioning of mouse corridor cells. By performing manipulations in E13.5 brain slices, we found that corridor cell migration is repelled by a ventral domain that includes the ventral MGE (vMGE) and anterior preoptic area (POA), which we will refer to as vMGE&POA (Figure S2). Indeed, using homotopic grafts of GFP-expressing LGE progenitors, we observed that ablations or dorsal grafts of vMGE&POA increased or limited, respectively, the ventral migration of corridor cells (Figure S2). In addition, we designed an in vitro assay in which we can confront vMGE&POA explants to mouse corridor cells, isolated in slice cultures on the basis of their ventral migratory route from the LGE (Figure S2). Although GFP-positive corridor cells migrated symmetrically from control explants cultured alone, they were reliably repelled by the vMGE&POA, when the explant was located at short distance (Figure S2). Thus, the mouse vMGE&POA produces a short-range repulsion for migrating corridor cells.

Because this activity is adequately located to shape the mouse corridor differentially from its chicken counterpart (Figures 4G, 4N, and S2), we searched for ventral repulsive cues differentially expressed in the two species. We focused on the secreted factor Slit2 because it is expressed in the midline of the mouse ventral telencephalon (Marillat et al., 2002; Nguyen Ba-Charvet et al., 1999). We observed that mouse *Slit2* is expressed in the ventricular zone of the vMGE&POA, with a dorsal limit of expression adjacent to the ventral tip of the corridor (Figure 5A). In contrast, chicken *cSlit2* expression is confined to the ventral midline and does not extend into the MGE domain, in which corridor cells converge (Figure 5D). Overall, our experiments identify Slit2 as a candidate factor to regulate the orientation of corridor cell migration.

Slit2 Is a Short-Range Repellent for Corridor Cell Migration

To investigate the role of Slit2 in corridor cell migration, we first examined the expression pattern of its receptors. In situ

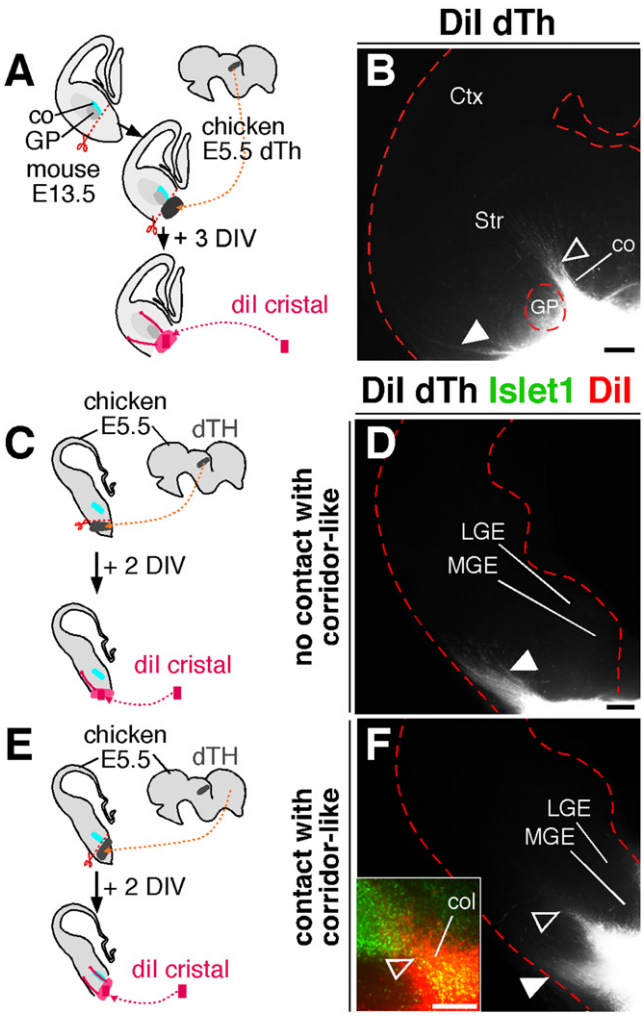

Figure 3. Chicken TAs Can Grow Internally in the Mouse or Chicken Corridor

(A and B) Experimental paradigm used to test the growth of chicken TAs in the mouse ventral telencephalon (A). Like mouse TAs ex vivo, DiI-labeled chicken TAs follow an internal (open arrowhead) and external path (solid arrowhead) in mouse slices (B).

(C–F) Experimental paradigm used to test the permissivity of the corridor-like structure (light blue) for chicken TAs. Chicken TAs follow an external path (solid arrowhead) when dTh explants have no contact with the corridor-like structure (D), whereas they also use an internal path (open arrowhead) when dTh explants are in contact with the corridor-like structure (F) (inset shows the contact between axons [red] and Islet1-positive corridor-like cells [green]).

Ctx, cerebral cortex; co, corridor; col, corridor-like; dTh, dorsal thalamus; Str, striatum. Scale bars, 100 μm (B), 50 μm (D and F), and 20 μm (inset in F).

hybridization alone or combined with Islet1 immunostaining (Lopez-Bendito et al., 2006) indicates that a large majority of mouse corridor cells express *Robo1* and *Robo2* transcripts (Figures 5B, 5C, and 5H–5I′). In addition, using embryonic brain slices in which LGE-derived cells are labeled with GFP, we found that migrating corridor cells express both Robo receptors at their surface (Figure 5G). Similarly, chicken corridor cells express *Robo1* and *Robo2* (Figures 5E and 5F), indicating that corridor cells may directly respond to Slit2 in both species.

To test next whether migrating corridor cells are sensitive to Slit2 activity, we grafted aggregates of control or *Slit2*-expressing COS cells into wild-type mouse slices containing GFP-expressing LGE cells (Figures 6A–6C). Corridor cells migrated close to control COS cells (n = 5) but remained at a short distance of *Slit2*-expressing COS cells (n = 11/12; Figures 6A–6C). Similar results were obtained when we electroporated the vMGE of chicken brain slices with control or *Slit2*-expressing plasmids, and monitored the migration of corridor cells by implanting a crystal of DiI in the LGE ($n_{control}$ = 7, n_{Slit2} = 7; Figures 6D–6F). Finally, we showed that Slit2 has a direct repulsive activity in corridor cell migration within a 275 μm radius, by confronting in vitro mouse corridor cell explants to control or *Slit2*-expressing COS cells (Figures 6G–6J; $n_{control}$ = 20, n_{Slit2} = 21). Thus, Slit2 exerts a short-range repulsive activity in the migration of both chicken and mouse corridor cells.

Because Slit2 is differentially expressed in mouse and chicken embryos, we wondered whether variations of *Slit2* expression might have an impact on the distribution of corridor cells in vivo. To this aim we performed in ovo electroporation of *GFP* control and *Slit2*-expression plasmids in the ventral telencephalon of E3 chicken embryos, and examined corridor cell distribution using Islet1 immunohistochemistry at E6 (Figures 6K–6N). We checked that we were accurately targeting the ventral telencephalon by examining *GFP* expression not only at E6, but also 20 hr post-electroporation, because the MGE and POA generate cells that colonize the entire ventral telencephalon (data not shown) (Cobos et al., 2001). Although *GFP* expression had no effect on the corridor (n = 16/16), we found that *Slit2* ectopic expression induced a mild change in the distribution of corridor cells, resulting in an overall visible modification of the corridor shape in the absence of other morphological defects (n = 13/13) (Figures 6M and 6N). Although these experiments are intrinsically variable, we reproducibly observed a change in the corridor shape of *Slit2*-electroporated embryos that resulted in a significant decrease of both the medial extension and the thickness of the corridor compared to the control situation (Figure 6L). Taken together, our results indicate that in ovo modifications of *Slit2* expression domain modify the distribution of the corridor, suggesting that *Slit2* repulsive activity participates to this process in vivo.

Slit2 Function Is Required to Orient the Migration of Mouse Corridor Cells

To further determine the role of Slit2 in the migration of corridor cells in vivo, we examined *Slit2* mutant mice (Plump et al., 2002). We first demonstrated using slice cultures that the repulsive activity of the vMGE&POA in corridor cell migration is abolished or drastically reduced in the absence of Slit2 function (Figure S3). To investigate whether *Slit2* inactivation affects the formation of the corridor, we performed a detailed in situ hybridization study in E13–E14.5 wild-type and mutant embryos, using a panel of molecular markers of corridor cells (*Ebf1*, *Meis2*, *Nrg1*), striatal neurons (*Ebf1*, *Meis2*, *Foxp2*) (Ferland et al., 2003), and of the surrounding MGE and POA-derived structures (*Lhx6*, *Nkx2.1*, *Shh*). In agreement with previous studies (Bagri et al., 2002; Marin et al., 2003), the general organization of the ventral telencephalon was normal in *Slit2*$^{-/-}$ embryos (Figure S4; data not

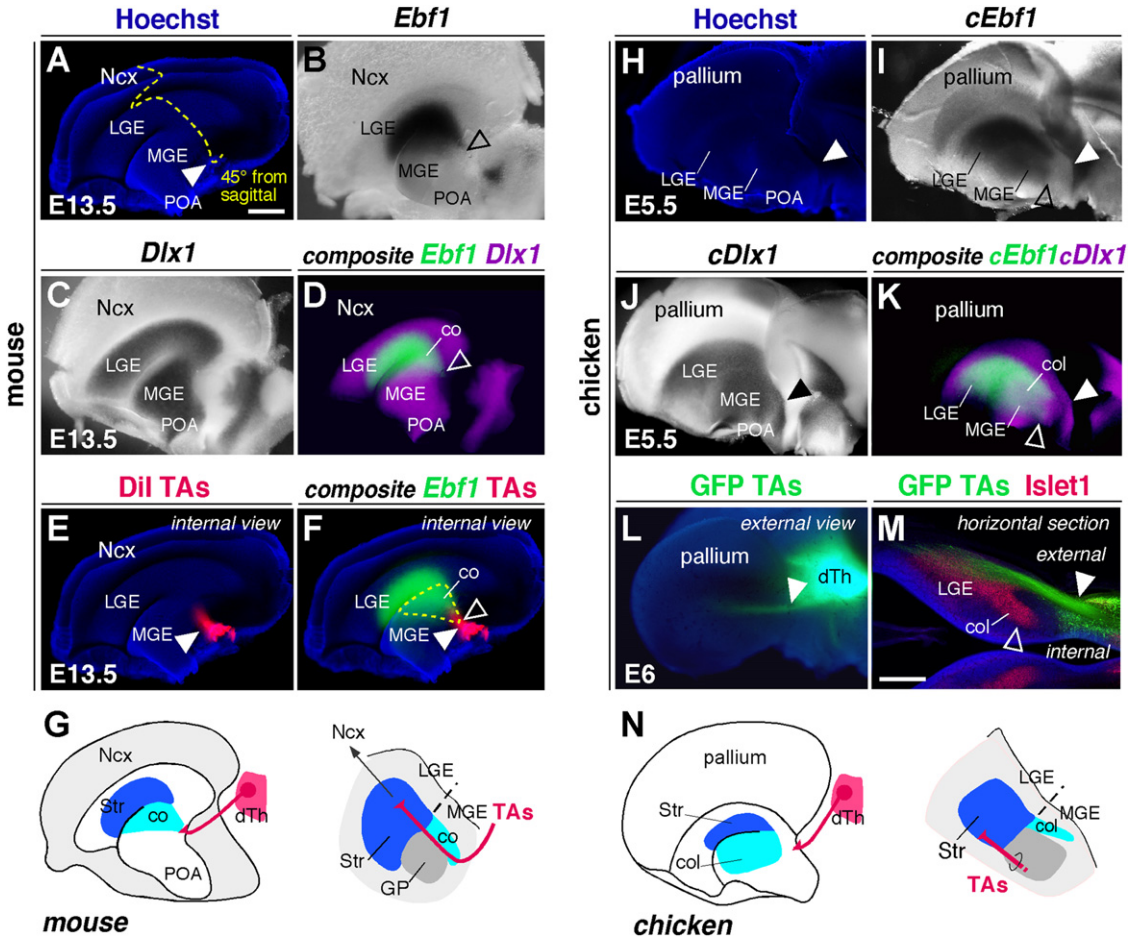

Figure 4. The Mouse and Chicken Corridor Have a Different 3D Organization

(A–F) Internal views of E13.5 mouse telencephalic vesicles showing nuclear staining (A), *Ebf1* expression to label the striatum and corridor (B), *Dlx1* expression to mark the ventral telencephalon (C), an artificial overlay of *Ebf1* and *Dlx1* in situ hybridization stainings *within* the ventral telencephalon (performed using morphological landmarks) (D), DiI labeling of TAs (E), and an artificial overlay of *Ebf1* expression and DiI labeling of TAs (performed as in D) (F). The *Ebf1*-labeled corridor expands to the caudomedial tip of the ventral telencephalon (open arrowhead in B, D, and F) where TAs enter (solid arrowhead in E and F), thereby allowing interactions between the corridor (yellow dots in F) and incoming axons. The dotted line in (A) marks the 45° angle section plane through which mouse TAs navigate.

(G) Schematic drawings representing the positioning of the mouse corridor and ingrowing TAs, in an internal telencephalic view (left) and in a 45° angle plane (right).

(H–K) Internal views of an E5.5 chicken telencephalic vesicle showing nuclear staining (H), *cEbf1* expression to label the striatum and corridor-like (I), *cDlx1* expression to mark the ventral telencephalon (J), and an artificial overlay of the two stainings, performed as in (D) (K). In contrast to the mouse, the chicken *Ebf1*-labeled corridor expands ventrally into the MGE (open arrowhead in I and K), remaining at a distance from the diencephalic/telencephalic boundary (solid arrowhead in H–K).

(L–M) External view (L) and horizontal section (M) of an E6 chicken embryo electroporated in the dorsal thalamus by a *GFP*-expressing plasmid. GFP-positive chicken TAs are only visible from an external view (L). Islet1 immunohistochemistry indicates that the corridor-like (open arrowhead in M) remains at a distance from the telencephalic/diencephalic boundary (solid arrowhead in L and M) where TAs enter the ventral telencephalon.

(N) Schematic drawings representing in chicken embryos the positioning of the corridor and ingrowing TAs, in an internal telencephalic view (left) and in a coronal plane (right).

co, corridor; col, corridor-like; dTh, dorsal thalamus; Ncx, neocortex; Str, striatum. Scale bars, 300 μm.

shown). However, we observed a three-dimensional distortion of the corridor in this mutant (Figures 7A–7H). In particular, as visualized by *Ebf1* expression in coronal and horizontal sections (n = 18), the mutant rostral corridor is wider, less compact, abnormally directed toward the ventral midline (Figures 7A–7H), and with ectopic *Ebf1*-expressing cells in the ventricular zone of the vMGE (Figures 7B and 7F). To quantify these morphological defects, we measured the medial extension and thickness of the rostral corridor in controls and mutant embryos, as we previously did in *Slit2* gain-of-function experiments in chicken embryos (Figures 6K–6N and S5). Consistently, we observed an opposite and significant increase in both the corridor medial expansion and thickness in mutant versus control embryos (Figure S5). In addition, the caudal extension of the corridor is severely reduced

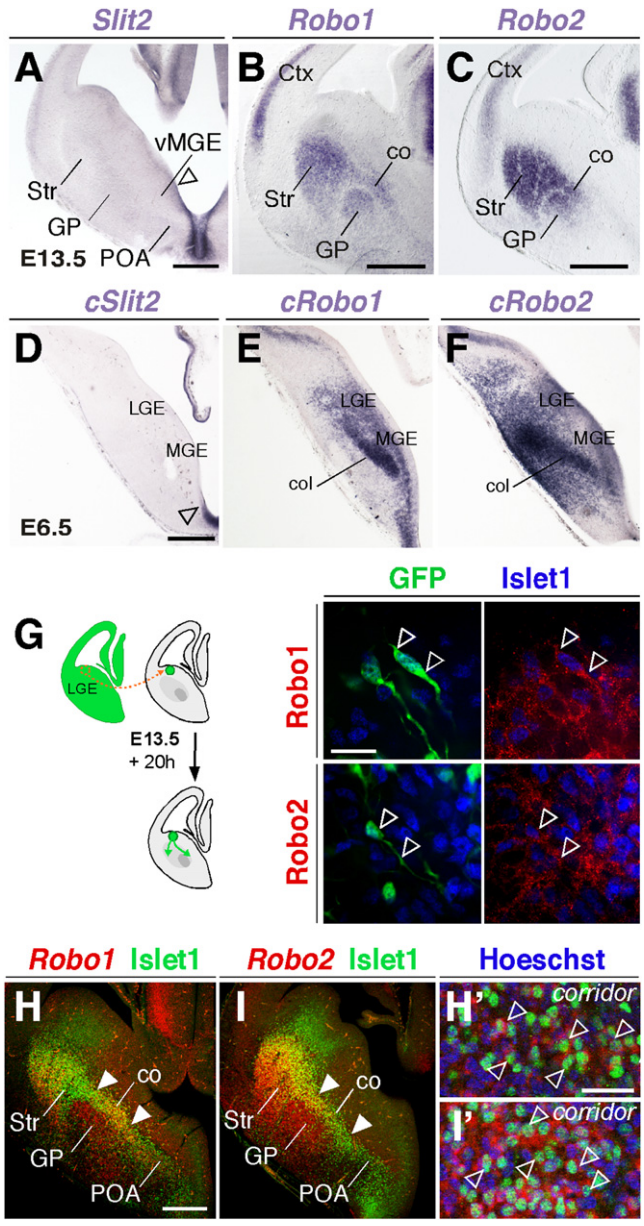

Figure 5. *Slit2* Is Differentially Expressed in Chicken and Mouse Embryos

(A–F) In situ hybridization on mouse (A–C) and chicken (D–F) coronal sections shows that *Slit2* expression in mouse embryos is located in the vMGE&POA (open arrowhead in A), whereas it is restricted to its ventral-most region in chicken embryos (open arrowhead in D), and *Robo1* and *Robo2* are expressed in the corridor region in both species (B, C, E, and F).

(G) Experimental design and colabeling of LGE-derived GFP-positive cells in the corridor, showing that migrating corridor cells have both ROBO1 and ROBO2 receptors on their surface (open arrowheads).

(H–I′) In situ hybridization and Islet1 immunohistochemistry show that the corridor region (solid arrowheads in H and I) expresses *Robo1* (H) and *Robo2* mRNAs (I) and that Islet1-positive corridor cells (open arrowheads) coexpress *Robo1* (H and H′) or *Robo2* (I and I′).

co, corridor; col, corridor-like; Ctx, cerebral cortex; Str, striatum. Scale bars, 300 μm (A–C), 200 μm (D–F), 10 μm (G), 300 μm (H and I), and 20 μm (H′ and I′).

or completely lacking in *Slit2*$^{-/-}$ embryos (Figures 7C, 7D, 7G, and 7H). Finally, because cortical axons converge toward the midline in these mutants (Bagri et al., 2002), we checked that the displacement of corridor cells occurs before cortical axonal pathfinding defects (Figure S6).

Overall, our results show that Slit2-mediated repulsion from the vMGE&POA controls the positioning of corridor cells. Indeed, in the absence of *Slit2* ventral repulsion (Figure S3), corridor cells collapse toward the vMGE midline at rostral levels, instead of continuing to migrate caudally (Figures 7A–7H). Furthermore, by examining single and double mutants for *Slit1*, *Slit1;Slit2*, *Robo1*, *Robo2*, and *Robo1;Robo2*, we found that this effect is specific of Slit2 and mediated by both Robo1 and Robo2 receptors (Figures S5 and S7).

Slit2 Inactivation Shifts TAs from an Internal to an External Path

Previous studies have shown that *Slit2* inactivation affects TA guidance (Bagri et al., 2002): some TAs fail to enter the telencephalon by invading the hypothalamus, and although some reach the striatum, the number of TAs reaching the neocortex at birth is severely reduced. Although *Slit2* expression in the hypothalamus prevents TAs from entering this structure (Bagri et al., 2002; Braisted et al., 2009), the mispositioning of corridor cells that we observed likely contributes to TA guidance defects in the ventral telencephalon of *Slit2* mutants.

To address this issue, we first analyzed the path of TAs in the corridor region of mutant embryos, which had not been examined before. We used a section plane that contains the entire path of TAs at E14 (45°, Figure 7D) and confirmed the lack of caudal corridor in mutant embryos (n = 4; Figures 7I and 7M). DiI labeling of TAs at E14.5 showed that they grow externally in mutant embryos in contrast to controls (n = 7; Figures 7J and 7N). Consistently, at E18.5, sensory TAs in *Slit2*$^{-/-}$ embryos follow a route external to the globus pallidus (GP), with only a very reduced number of axons reaching the neocortex (n = 6; Figures 7K and 7O; data not shown). This phenotype was observed before TAs interacted with corticofugal axons and before any defects in cortical axons were detected in mutant embryos (Bagri et al., 2002) (Figure S6). Thus, in *Slit2*$^{-/-}$ embryos, in which corridor cells are misplaced, TAs undertake external alternative paths (Figures 7L and 7P), a situation highly reminiscent of the chicken embryo.

Slit2 Controls the Internal Path of TAs via Corridor Cell Positioning

Because TAs express Robo1 and 2 receptors and are repelled by Slit2 (Braisted et al., 2009; Lopez-Bendito et al., 2007), these pathfinding defects could be due either to a direct effect of Slit2 on axons and/or to an indirect effect via corridor cell positioning. To determine the relative contribution of these modes of Slit2 activity, we first tested using slice culture experiments whether the lack of Slit2/Robo signaling in TAs directly affects their pathfinding (Figure S8). When wild-type thalamic explants are grafted in *Slit2*$^{-/-}$ coronal slices, TAs grew into the mutant corridor, even though Slit2 is lacking in host slices ($n_{control}$ = 12, $n_{Slit2-/-}$ = 12; Figure S8). Thus, consistent with *Nrg1* expression in mutant embryos (data not shown), *Slit2* inactivation does not affect the

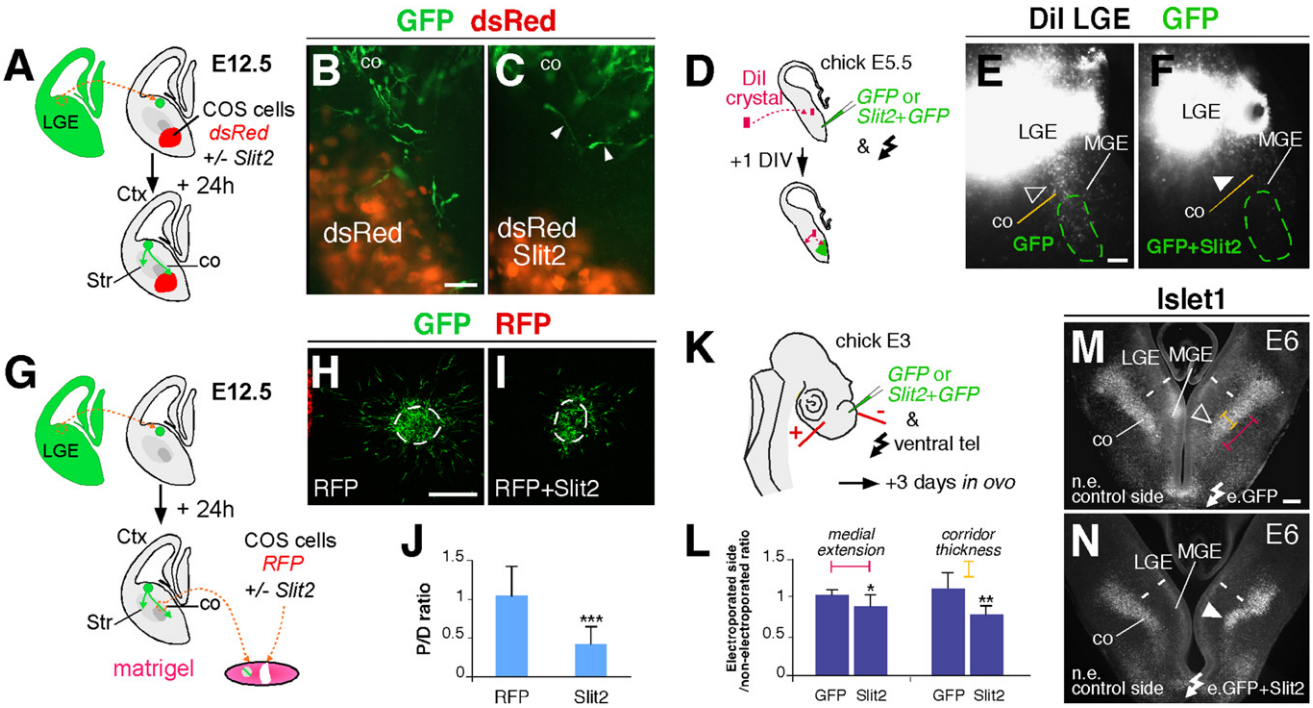

Figure 6. Slit2 Acts as a Short-Range Repellent on the Migration of Corridor Cells

(A–C) Experimental paradigm used to test the activity of Slit2 in corridor cell migration in cultured mouse embryonic brain slices (A). GFP-expressing corridor cells migrated close to control COS cells (B) but remained at a distance (arrowheads) from *Slit2*-expressing COS cells (C).

(D–F) Experimental paradigm used to test the activity of Slit2 in chicken corridor cell migration (D). LGE DiI-labeled migrating cells (open arrowhead) enter the MGE after the ectopic expression of *GFP* in the MGE (green outline shows the site of electroporation) (E) but do not migrate into the MGE after the ectopic expression of *Slit2* and *GFP* (F) (solid arrowhead) (green dashes outline the electroporation site).

(G–J) Experimental paradigm used to test the activity of Slit2 in corridor cell migration in Matrigel (G). GFP immunocytochemistry shows that corridor cells migrate radially when facing control COS cells (H) and tend to avoid *Slit2*-expressing COS cells (I). This repulsive effect is significant, as quantified by proximal/distal ratio ($P/D_{control}$ = 1.05 ± 0.37; P/D_{Slit2} = 0.43 ± 0.22; $p < 10^{-6}$) (J).

(K and L) Experimental paradigm used to test the effect of *Slit2* in ovo electroporation in the ventral telencephalon of chicken embryos (K). *GFP* electroporation does not modify the shape of the corridor (open arrowhead in M) as visualized by comparison of Islet1 immunostaining on nonelectroporated (n.e., left) and electroporated (e., right) sides on E6 coronal sections (M). In contrast, *Slit2* electroporation perturbs corridor cell distribution (solid arrowhead in N) reflected by a compacted and less extended Islet1 immunostaining on the electroporated side (solid arrowhead in N). Quantification of the corridor medial extension (pink bracket in M) and thickness (yellow bracket in M) as ratios between the electroporated and nonelectroporated sides shows that *Slit2* electroporation leads to a significant decrease in both parameters, which is consistent with a repulsive activity of the factor (L) ($ratio_{E./N.E.GFP}$ = 1.01 ± 0.07 and 1.08 ± 0.20; $ratio_{E./N.E.Slit2}$ = 0.86 ± 0.15 and 0.78 ± 0.12; $p < 0.02$ and $p < 2.10^{-5}$ for medial extension and thickness, respectively).

co, corridor; Ctx, cerebral cortex; Str, striatum. Scale bars, 50 μm (B and C), 20 μm (E and F), 150 μm (I and J), and 200 μm (N and O). *$p < 0.05$; **$p < 0.005$; ***$p < 0.001$.

guidance properties of corridor cells. Conversely, *Robo1*$^{-/-}$;*Robo2*$^{-/-}$ TAs (Grieshammer et al., 2004; Long et al., 2004; Ma and Tessier-Lavigne, 2007) navigate into the corridor of a wild-type coronal slice ($n_{control}$ = 6, $n_{Robo1-/-;Robo2-/-}$ = 13; Figure S8). Taken together, these experiments show that *Slit2* expression within the ventral telencephalon does not directly control TA internal/external pathfinding. To further test the role of *Slit2* hypothalamic expression, we grafted *Robo1*$^{-/-}$;*Robo2*$^{-/-}$ thalamic explants in 45° angle wild-type slices that contain the entire axonal pathway as well as the hypothalamus (Figures 7D and 7L). Although some *Robo1*$^{-/-}$;*Robo2*$^{-/-}$ mutant TAs abnormally entered the hypothalamus (n = 6/9; Figure S8), thereby confirming the role of *Slit2* in this region (Braisted et al., 2009), mutant axons that entered the ventral telencephalon followed an internal path similar to wild-type axons ($n_{control}$ = 18, $n_{Robo1-/-;Robo2-/-}$ = 9; Figure S8). Thus, whereas Slit2 prevents TAs from entering the hypothalamus, it does not have a major direct activity in TA positioning within the ventral telencephalon.

To address if Slit2 acts indirectly on TAs via corridor cell positioning, we tested whether grafting a wild-type corridor into *Slit2*$^{-/-}$ mutant slices would be sufficient to rescue TA pathfinding defects in mutant embryos (Figures 8A–8G). To this end, we used 45° angle slices that contained the entire axonal pathway (Figures 7J and 8A–8C), in which we performed an initial cut at the border between the ventral telencephalon and diencephalon (Figures 8A–8C). As observed in vivo (Figures 7J and 7N), TAs turned internally into the corridor in wild-type slices (n = 10; 84% ± 13% of dorsal axons; Figures 8D and 8G), whereas they grew externally in *Slit2* mutant slices (n = 10; 22% ± 14% of dorsal axons; Figures 8E and 8G). Strikingly, in *Slit2*$^{-/-}$ slices in which we grafted a wild-type GFP-expressing corridor, TA pathfinding was rescued in 71% of cases (n = 10/14),

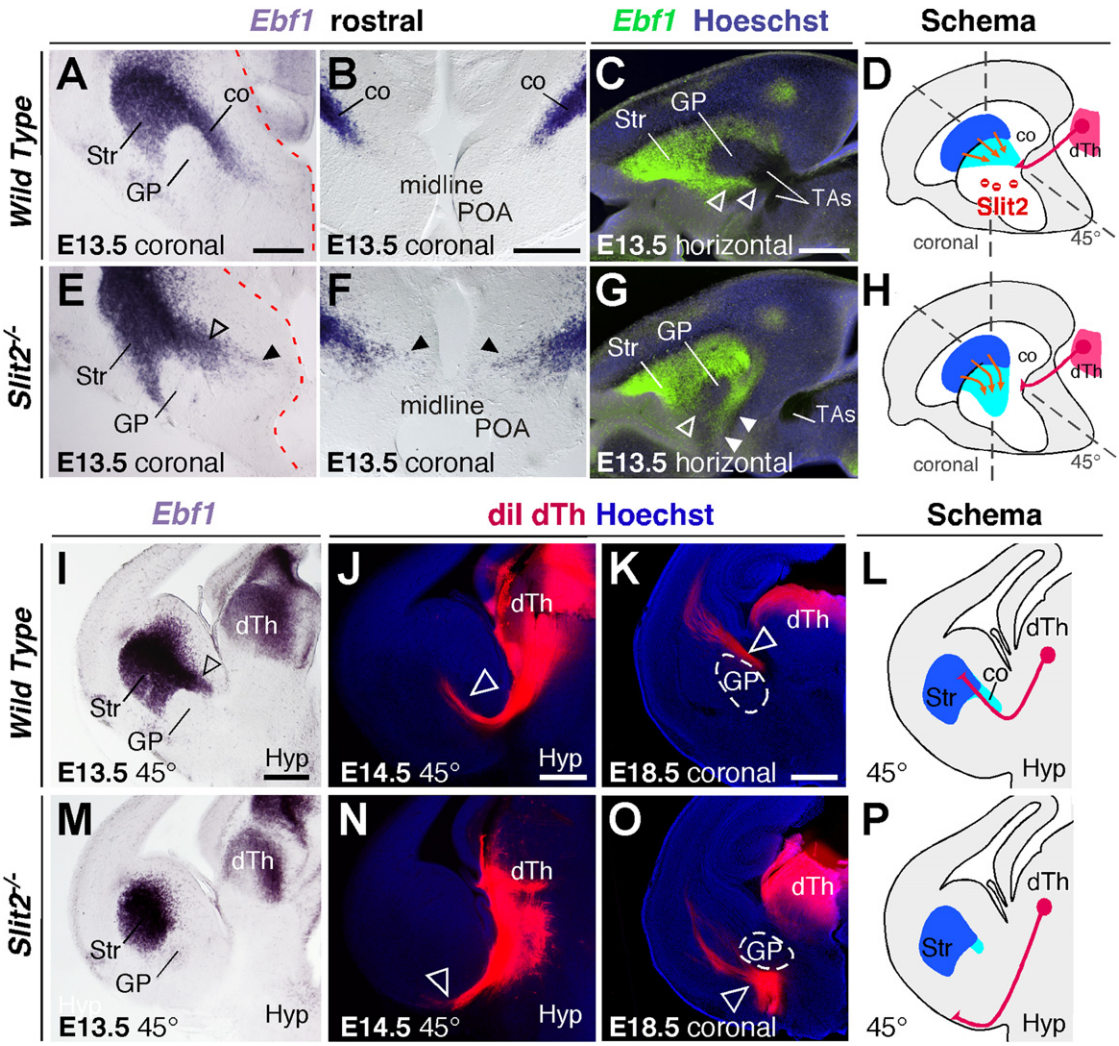

Figure 7. Distorted Corridor and Alternative Path of TAs in *Slit2*$^{-/-}$ Mutants

(A–C and E–G) *Ebf1* expression on E13.5 rostral coronal sections (A, B, E, and F) and on horizontal sections (C and G). Contrary to wild-type embryos (A–C), *Ebf1*-expressing cells in *Slit2* mutants are detected in a domain converging toward the midline (open arrowhead) with ectopic cells near the midline (solid arrowheads) (E–G). On horizontal sections, the *Ebf1*-positive corridor is distorted toward the rostral midline in *Slit2*$^{-/-}$ embryos (open and solid arrowheads), leaving a gap between the caudal end of the corridor and ingrowing TAs (C and G).

(D and H) Schematic representations showing that the wild-type corridor (co, light blue) has a fan shape with a caudomedial tip (D), whereas the mutant corridor is oriented toward the midline (H). TAs (pink) are either in vicinity of corridor cells in wild-type embryos or at a distance in *Slit2*$^{-/-}$ mutants. Gray-dotted lines indicate the coronal and 45° planes used in the top and bottom panels.

(I and M) *Ebf1* expression on 45° sections showing the presence (I) and the absence (M) of a caudal corridor (open arrowhead) in wild-type and *Slit2*$^{-/-}$ embryos, respectively.

(J, K, N, and O) Tracing by DiI injections at E14.5 (45° sections, plane as in I and M) and E18.5 (coronal sections) shows that TAs follow an internal route (open arrowheads) in wild-type embryos (J and K) versus an external path (solid arrowheads) in *Slit2*$^{-/-}$ embryos (N and O).

(L and P) Schematic representations showing the position of corridor cells and TAs in control and *Slit2*$^{-/-}$ embryos.

co, corridor; dTh, dorsal thalamus; Hyp, hypothalamus; Str, striatum. Scale bars, 300 μm, except 500 μm for (K) and (O).

with significantly more TAs turning dorsally into an internal path than with only a control incision (68% ± 16% of dorsal axons; $p < 10^{-5}$; Figures 8F and 8G). These results demonstrate that, in the absence of Slit2, the caudal introduction of a corridor is sufficient to reorient TA growth along an internal versus an external path. It should also be mentioned that all TAs were not rescued by the grafting experiment, indicating that a direct action of Slit2 on axons might additionally increase the reliability of TA pathfinding in the ventral telencephalon. Thus, our results show that Slit2 activity in TA navigation within the MGE is primarily mediated by the positioning of migrating guidepost corridor neurons.

Overall, our experiments show that Slit2 acts as a repellent to control the positioning of the corridor, which in turn is required to switch TAs from an external path to an internal path (Figure 8H).

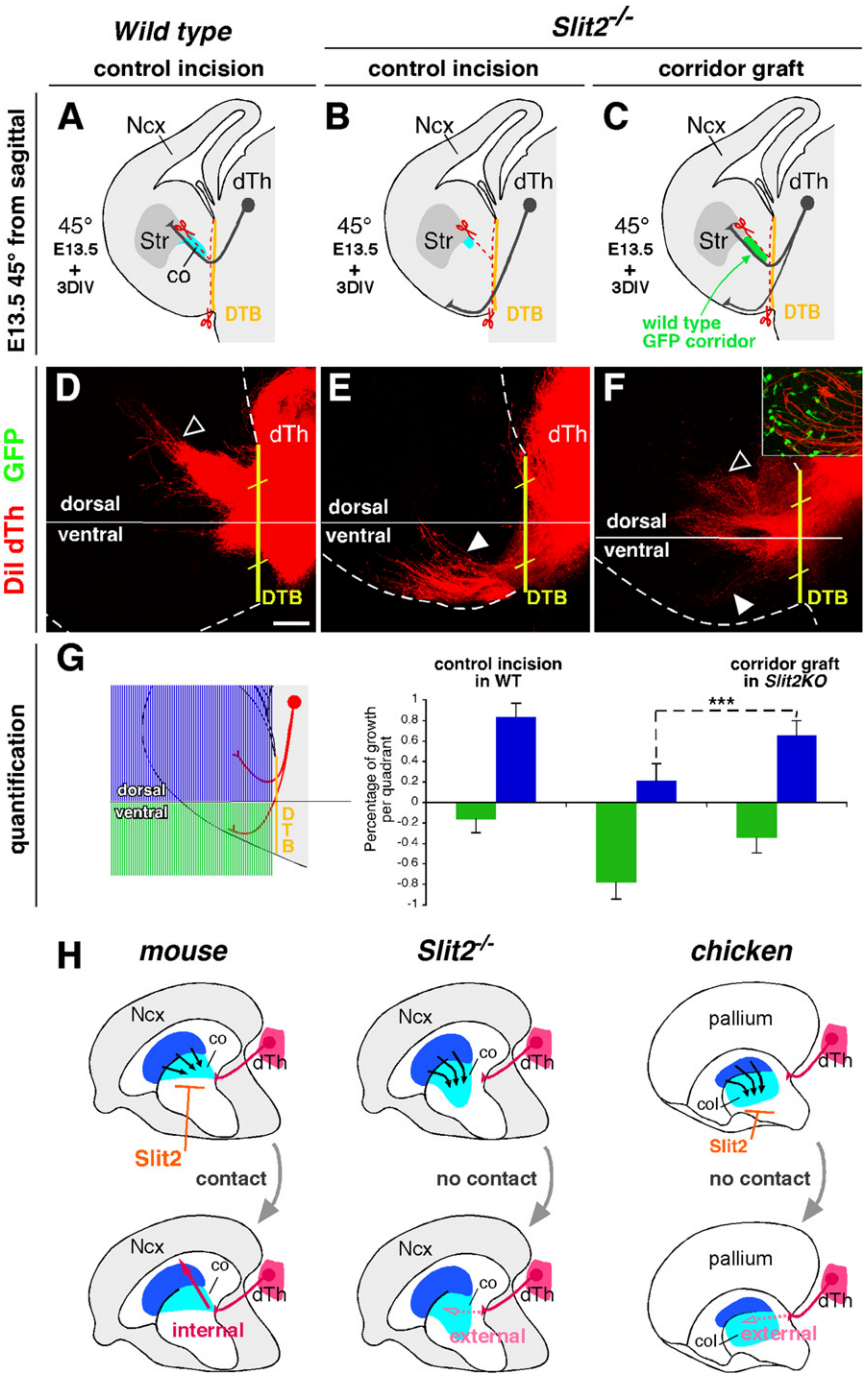

Figure 8. Homotopic Graft of a Wild-Type Corridor Is Sufficient to Rescue an Internal Pathfinding of TAs in *Slit2*$^{-/-}$ Brain Slices

(A–C) Experimental paradigm used to label TA trajectory in wild-type (A) and *Slit2*$^{-/-}$ (B) cultured slices (45° between sagittal and coronal) and to test the rescue of TA pathfinding in *Slit2*$^{-/-}$ cultured slice by homotopic graft of a GFP-expressing wild-type corridor (C).

(D and E) TA tracing by DiI injection after culture showing the internal path of TAs in wild-type slices (open arrowhead) (D) and the external path in *Slit2*$^{-/-}$ slices (solid arrowhead) (E).

(F) TA tracing by DiI injection after culture showing that most TAs choose an internal path (open arrowhead) by interacting with GFP-grafted cells (inset), whereas a limited number of axons still follow an external path (solid arrowhead).

(G) Quantification of axonal growth per dorsal and ventral quadrant in experiments similar to (D)–(F) showing that the graft of a wild-type corridor efficiently rescues the pathfinding of TAs in *Slit2*$^{-/-}$ slices (dorsal $axons_{controls}$ = 84% ± 13%; dorsal $axons_{Slit2-/-}$ = 22% ± 14%; dorsal $axons_{Grafted\ Slit2-/-}$ = 68% ± 16%; $p < 10^{-5}$).

(H) Model of Slit2 activity in the positioning of TAs. At early stages (top panels), the migration of corridor cells (black arrows) is differentially oriented by the expression of *Slit2* in mouse embryos or its local/total absence in chicken or *Slit2* mutant embryos. This differential positioning of corridor neurons allows or precludes a future contact with TAs. At later stages (bottom panels), mammalian corridor cells provide leverage for an internal trajectory of TAs to the neocortex, in contrast to the default external path observed in *Slit2* mutant mice or chicken embryos.

co, corridor; col, corridor-like; DTB, diencephalic/telencephalic boundary; dTh, dorsal thalamus; Ncx, neocortex; Str, striatum. Scale bars, 100 μm. ***$p < 0.001$.

DISCUSSION

In this study we have shown that the orientation of corridor cells migration shapes the opening of a mammalian internal path for TAs different from a default external path characteristic of reptiles and birds. At the molecular level, Slit2/Robo signaling orients the migration of these guidepost neurons and thereby indirectly controls the dorsoventral navigation of TAs (Figure 8H). Thus, our work demonstrates that the local modulation of neuronal migration at intermediate targets by Slit2 triggers the large-scale remodeling of a major axonal projection and opens perspectives on the evolution of brain connectivity.

Positioning of Guidepost Neurons by Migration Shapes the Trajectory of TAs

Although the mechanisms controlling axon guidance are highly conserved in vertebrates and invertebrates, how axonal tracts have evolved in distinct species remains largely unknown. Embryological and comparative studies have suggested that most changes in axonal tracts may occur by the use of preexisting pathways, whereas the development of others, such as the corpus callosum, which interconnects the two cortical hemispheres in mammals, may have emerged through the formation of a novel substrate (Katz et al., 1983). Thalamic projections, which provide the main input to the mammalian neocortex, have undergone

a major change in trajectory during the evolution of tetrapods, from an external peduncle to an internal capsule. In this study, we show that species-specific differences in the migration of guidepost neurons with conserved guidance properties constitute an essential step in the opening of an internal trajectory for TAs to the neocortex. We had previously shown that TA pathfinding through the mouse ventral telencephalon is delineated by a permissive corridor generated by tangential neuronal migration (Lopez-Bendito et al., 2006), raising the question of how such an apparently complex process may emerge during evolution. By performing comparative studies, we have now revealed that corridor-like cells are conserved in reptiles/birds, similar to other neuronal populations of the internal capsule (Cordery and Molnar, 1999), although they do not act as guidepost cells for TAs in these species. Using the chicken embryo as an experimental model, we have shown that corridor-like cells share all the intrinsic characteristics of their mouse homologs (Lopez-Bendito et al., 2006), including a remarkably similar capacity to guide TAs, but these neurons converge toward the midline and, hence, are never in contact with TAs in vivo. Thus, the specification and overall migration of corridor-like cells seem independent of their role in TA guidance, thereby suggesting that these neurons may exert other ancestral functions and that their guidepost function for TAs has been acquired secondarily.

Most importantly, our observations indicate that a cardinal difference between living reptiles and mammals lays in the orientation of migration of neurons that have the cellular capacity to guide TAs. Furthermore, using *Slit2*$^{-/-}$ mutant mice, we showed that the proper positioning of corridor cells by migration is required and sufficient to switch TAs from an external default path to a mammalian internal route (Figure 8H). Thus, the corridor acts in mice as an anatomical "hotspot" in which local changes in cell migration have long-range and large-scale effects on the guidance of TAs. Taken together, our experiments strongly support a surprising evolutionary scenario in which changes in the migration of intermediate neurons have provided an opportunity for the opening of a major axonal highway.

Slit2 Activity in the Migration of Guidepost Cells Controls TA Trajectory

To unravel the molecular mechanisms underlying the evolutionary change in corridor neuron migration, we focused on the secreted factor Slit2. In this study we showed that (1) *Slit2* is differently expressed in the vMGE&POA of mouse and chicken embryos; (2) Slit2 acts as a short-range repellent on the migration of corridor cells; (3) modifying *Slit2* levels in the ventral telencephalon of chicken embryos distorts the shape of the corridor; and (4) *Slit2* inactivation impairs the mammalian-specific migration of corridor neurons by shifting them toward the midline, a behavior reminiscent of chicken corridor-like cells. These results reveal that Slit2 is a major determinant in the orientation of mouse corridor neuron migration, by acting at short-range from the vMGE&POA, and thereby controls TA trajectory. Thus, in contrast to a direct role of Slit2 on axonal navigation (Bagri et al., 2002; Braisted et al., 2009; Nguyen-Ba-Charvet et al., 2002; Shu et al., 2003b), our study provides a different mechanism of Slit function on longitudinal axonal positioning through a short-range activity in guidepost cell migration. This relay of midline signaling by an early and, thus, local activity in intermediate target cells may more generally explain how midline cues can act at long range in very large structures, such as the mammalian telencephalon.

Furthermore, our comparative analysis suggests that local variations in the expression domain of *Slit2* contributed to the evolutionary modification of a major axonal tract. Minor changes in early patterning events have been shown to underlie large-scale morphogenetic rearrangements of the body plan (Carroll, 2008). Consistently, relatively small variations in Shh and Wnt signaling pathways participated in the rapid evolution of the brain in fish populations located in distinct natural environments (Menuet et al., 2007; Sylvester et al., 2010). Our results open the intriguing possibility that similar mechanisms may have governed the evolution of brain connectivity, via local changes in the expression of highly conserved guidance cues. What may modulate *Slit2* expression in distinct species? One possibility is that upstream transcriptional regulators of *Slit2* may be differentially expressed in mammals and reptiles/birds. A nonexclusive alternative is that *Slit2 cis*-regulatory sequences may have undergone evolutionary changes, leading to species-specific variations in gene expression. It has been shown that modifications of *cis*-regulatory sequences constitute a powerful drive for the evolution of complex patterns by modulating spatially and temporally the transcriptional regulation of conserved genetic cascades (Carroll, 2008). Therefore, it will be of great interest to investigate whether similar mechanisms are involved in the species-specific expression of *Slit2*, and may thus have participated in the evolution of brain wiring.

Neuronal Migration of Guidepost Cells in the Evolution of Cortical Connectivity

The telencephalon of vertebrates has undergone major changes that include a quantitative increase in both neurogenesis and cell migration, and which have led to the development of the six-layered neocortex of living mammals (Kriegstein et al., 2006). If the emergence of the neocortex is directly related to intrinsic changes in the dorsal telencephalon, it is also linked to global modifications of connectivity, such as the appearance of a large internal capsule. Our study shows that small changes in neuronal cell migration at intermediate targets have been essential to create an opportunity for this axonal highway, acting in parallel with cortical evolution to promote the functional emergence of the mammalian neocortex.

What may be the selective advantages of an internal trajectory of TAs? First, the internal path is associated with the formation of a large fan-shaped thalamic projection that radiates along the entire rostrocaudal axis as it enters the telencephalon. This feature is highly divergent from the reptilian TAs, which navigate as a compact axonal tract as they enter the subpallium. As such, the internal path may allow both the channeling of a large number of axons directly to the neocortex—creating an axonal highway—as well as the early "spreading" of thalamic projections and the entire covering of an expanding mammalian neocortex—creating a capsule versus a peduncle. In addition, the internal path constitutes a shorter thalamocortical pathway than an external one, thereby providing a faster route for the

transfer of information that may have favored the neocortical expansion.

Furthermore, our study opens the possibility that changes in cell migration may more generally participate in the evolution of brain connectivity. Consistently, it was shown that the formation of the corpus callosum, a mammalian-specific tract, relies on the migration of guidepost neurons (Shu et al., 2003a; Niquille et al., 2009). Indeed, the mammalian telencephalon is characterized by a complex choreography of tangential neuronal migrations originating in both dorsal and ventral regions, which is essential for its functioning because cell migration defects have been involved in the etiology of several pathologies (McManus and Golden, 2005). Thus, our study raises the intriguing possibility that tangential neuronal migrations may have promoted the evolution of the telencephalon at the expense of its developmental robustness.

EXPERIMENTAL PROCEDURES

Mouse Lines

Wild-type and GFP-expressing transgenic mice (Hadjantonakis et al., 1998), maintained in Swiss OF1 background, were used for expression analysis and tissue culture. *Slit1*$^{-/-}$, *Slit2*$^{-/-}$, and *Slit1*$^{-/-}$;*Slit2*$^{-/-}$ mutant embryos were obtained by crossing *Slit1*$^{+/-}$, *Slit2*$^{+/-}$, and *Slit1*$^{-/-}$;*Slit2*$^{+/-}$ parents (Plump et al., 2002) maintained in B6D2 background. *Robo1*$^{-/-}$, *Robo2*$^{-/-}$, and *Robo1*$^{-/-}$;*Robo2*$^{-/-}$ were obtained by crossing *Robo1*$^{+/-}$, *Robo2*$^{+/-}$, and *Robo1*$^{+/-}$;*Robo2*$^{+/-}$ parents (Grieshammer et al., 2004; Long et al., 2004; Ma and Tessier-Lavigne, 2007), which were maintained in CD1, C57BL/6, and mixed CD1–C57BL/6 backgrounds, respectively. Animals were kept under French and EU regulations.

Preparation of Other Tissues

Chinese soft-shelled turtle embryos (Nagashima et al., 2009) and corn-snake embryos (Gomez et al., 2008) were fixed in 4% paraformaldehyde (PFA) for 24–48 hr, kept in methanol, rehydrated, and cut into 100 μm thick sections on a vibratome. Sheep embryo was obtained by permission from a slaughterhouse in Cartagena (Spain), perfused with 4% PFA, postfixed overnight, embedded in paraffin, and cut into 8 μm sections. Human embryos were obtained from legal abortions (procedure approved by the French National Ethical Committee CCNESVS), staged, fixed in 4% PFA, cryoprotected, and cut into 12 μm thick sections as described previously (Verney et al., 2001).

In Situ Hybridization, Immunohistochemistry, and Axonal Tracing

For in situ hybridization, mouse or chicken brains were fixed overnight in 4% PFA in PBS. Twenty micrometer frozen sections or 80 μm free-floating vibratome sections were hybridized with digoxigenin-labeled probes as described before (Lopez-Bendito et al., 2006). For immunohistochemistry, cultured slices/explants and mouse or chicken embryos were fixed in 4% PFA at 4°C for 30 min and for 2–3 hr, respectively. Immunohistochemistry was performed on culture slices, Matrigel pads, and 100 μm free-floating vibratome sections as previously described (Lopez-Bendito et al., 2006) using the following antibodies: mouse anti-β3-Tubulin 1/1000 (Promega); rabbit anti-GFP 1/500 (Molecular Probes); mouse anti-Islet1 39.4D5 1/100 (Developmental Studies Hybridoma Bank [DSHB]); rabbit anti-Nkx2-1 1/2000 (BIOPAT); rat anti-L1 1/200 (Millipore); goat anti-Robo1 and anti-Robo2 1/100 (R&D Systems); mouse anti-neurofilament 2H3 1/100 (DSHB); mouse anti-TAG-1(4D7) 1/50 (DSHB); mouse anti-chicken TAG-1(23.4-5) 1/50 (DSHB); and rabbit anti-Tyrosine hydroxylase 1/100 (Pel-Freez). The colocalization of signals at a cellular scale was investigated by confocal section acquired on a spinning disk confocal system (DM5000B, Leica; CSU10,Yokogawa; HQ2,CoolSNAP) (Figures 5 and S1). For axonal tracing, embryonic brains or cultured slices were fixed overnight or for 30 min in 4% PFA, respectively. Small DiI crystals (1,1'-dioctadecyl 3,3,3′,3′-tetramethylindocarbocyanine perchlorate; Molecular Probes) were inserted, and after diffusion at 37°C, brains were cut on a vibratome into 80–100 μm sections. Hoechst (Sigma) or SYTOX Green (Molecular Probes) was used for nuclear counterstaining.

Slice and Explant Culture Experiments

Organotypic slice cultures of embryonic mouse or chicken brains were performed as previously described (Lopez-Bendito et al., 2006). Aggregates of COS7 cells, transfected with a myc-tag human *Slit2* expression vector (Brose et al., 1999) and/or *RFP/DsRed*-expression plasmids (Lipofectamine 2000, Invitrogen; FuGene 6, Roche), were prepared by diluting transfected cells in Matrigel (Lopez-Bendito et al., 2006) or by hanging drop (Wu et al., 1999).

Ex Vivo and In Ovo Focal Electroporation

Focal slice electroporations of *Gfp* and *Slit2* expression vectors (Brose et al., 1999) in the MGE were performed as previously described (Lopez-Bendito et al., 2006) using a pneumatic pump Inject+Matic (Inject+Matic, Switzerland) and a setup of horizontal platinum electrodes (Nepa Gene, Japan) powered by a CUY21 Edit (Nepa Gene, Japan). The telencephalic ventricle of E3 chicken embryos was injected with a DNA solution (2.0 or 2.5 μg/μl) and electroporated using the CUY21 Edit (eight 50 ms pulses of 30 V) (Alexandre et al., 2006).

Statistical Methods

The asymmetry of cell migration (Figures 6 and S2) was analyzed in 120° wide proximal and distal quadrants centered on explants localized at less than 275 μm of the source. The distance between cells and the center of the explant was measured, and the proximal/distal ratio was calculated between the sum of distances in the proximal and in the distal quadrant. To quantify axonal growth in the dorsal and ventral quadrants (Figure 8), nonsaturated DiI signal was acquired on a spinning disk confocal system, and an ImageJ plug-in was used to integrate the DiI intensity in each quadrant. A ratio of integrated intensity was calculated between the dorsal and ventral quadrants. All statistical analyses are presented as mean ± standard deviation. The p values were determined by Student's two-tailed t test except for Figures 6L and S5, where p values were determined by ANOVA test, followed by pairwise t tests with Benjamini and Hochberg adjustments.

SUPPLEMENTAL INFORMATION

Supplemental Information includes Supplemental Experimental Procedures and eight figures and can be found with this article online at doi:10.1016/j.neuron.2011.02.026.

ACKNOWLEDGMENTS

We are grateful to Patrick Charnay for his hospitality at the beginning of this work, to Alain Chedotal for the generous gifts of plasmids and reagents, and to Marion Wassef for her insightful discussions and input on the manuscript. We thank Alessandra Pierani and Xavier Morin for their critical comment during the course of this work and on the manuscript, and Alain Prochiantz for stimulating scientific discussions. We are grateful to Victor Borrell and Isabel Reillo for the kind gift of sheep embryo sections, to Shigeru Kuratani and Hiroshi Nagashima for the kind gift of Chinese soft-shelled turtle embryos, to Olivier Pourquié and Nicolas Denans for the kind gift of corn-snake embryos, and to Christine Métin for sharing unpublished results. We thank Noelia Garcia, Benjamin Mathieu, and Deborah Souchet for excellent technical assistance. We are grateful to members from the Garel and López-Bendito labs for stimulating discussions and ideas, and to members of the Charnay lab, Brunet/Goridis lab, Pierani lab, and Wassef lab for discussions and the gift of plasmids and reagents. This work was supported by grants from the INSERM "Avenir" Program to S.G., the City of Paris to S.G., the ARC to S.G., the FRC to S.G., and the EURYI program to S.G.; by grants from the Spanish Ministry of Science and Innovation BFU2006-00408/BFI and BFU2009-08261 to G.L.-B., and CONSOLIDER CSD2007-00023 to G.L.-B.; and by the PAI Picasso and Acciones Integradas to S.G. and G.L.-B. F.B. was supported by a fellowship from the French Ministry of Research. P.M.-M. was supported by a FPI fellowship from the Spanish Ministry of Science and Innovation. S.G. is a EURYI Awardee.

Accepted: January 13, 2011
Published: March 23, 2011

REFERENCES

Alexandre, P., Bachy, I., Marcou, M., and Wassef, M. (2006). Positive and negative regulations by FGF8 contribute to midbrain roof plate developmental plasticity. Development *133*, 2905–2913.

Andrews, W., Liapi, A., Plachez, C., Camurri, L., Zhang, J., Mori, S., Murakami, F., Parnavelas, J.G., Sundaresan, V., and Richards, L.J. (2006). Robo1 regulates the development of major axon tracts and interneuron migration in the forebrain. Development *133*, 2243–2252.

Auladell, C., Perez-Sust, P., Super, H., and Soriano, E. (2000). The early development of thalamocortical and corticothalamic projections in the mouse. Anat. Embryol. (Berl.) *201*, 169–179.

Bagri, A., Marin, O., Plump, A.S., Mak, J., Pleasure, S.J., Rubenstein, J.L., and Tessier-Lavigne, M. (2002). Slit proteins prevent midline crossing and determine the dorsoventral position of major axonal pathways in the mammalian forebrain. Neuron *33*, 233–248.

Braisted, J.E., Tuttle, R., and O'Leary, D.D.M. (1999). Thalamocortical axons are influenced by chemorepellent and chemoattractant activities localized to decision points along their path. Dev. Biol. *208*, 430–440.

Braisted, J.E., Ringstedt, T., and O'Leary, D.D.M. (2009). Slits are chemorepellents endogenous to hypothalamus and steer thalamocortical axons into ventral telencephalon. Cereb. Cortex *19* (*Suppl 1*), i144–i151.

Braisted, J.E., Catalano, S.M., Stimac, R., Kennedy, T.E., Tessier-Lavigne, M., Shatz, C.J., and O'Leary, D.D.M. (2000). Netrin-1 promotes thalamic axon growth and is required for proper development of the thalamocortical projection. J. Neurosci. *20*, 5792–5801.

Brose, K., Bland, K.S., Wang, K.H., Arnott, D., Henzel, W., Goodman, C.S., Tessier-Lavigne, M., and Kidd, T. (1999). Slit proteins bind Robo receptors and have an evolutionarily conserved role in repulsive axon guidance. Cell *96*, 795–806.

Butler, A.B. (1994). The evolution of the dorsal thalamus of jawed vertebrates, including mammals: Cladistic analysis and a new hypothesis. Brain Res. Brain Res. Rev. *19*, 29–65.

Carroll, S.B. (2008). Evo-devo and an expanding evolutionary synthesis: A genetic theory of morphological evolution. Cell *134*, 25–36.

Cobos, I., Puelles, L., and Martinez, S. (2001). The avian telencephalic subpallium originates inhibitory neurons that invade tangentially the pallium (dorsal ventricular ridge and cortical areas). Dev. Biol. *239*, 30–45.

Cordery, P., and Molnar, Z. (1999). Embryonic development of connections in turtle pallium. J. Comp. Neurol. *413*, 26–54.

Farmer, W.T., Altick, A.L., Nural, H.F., Dugan, J.P., Kidd, T., Charron, F., and Mastick, G.S. (2008). Pioneer longitudinal axons navigate using floor plate and Slit/Robo signals. Development *135*, 3643–3653.

Ferland, R.J., Cherry, T.J., Preware, P.O., Morrisey, E.E., and Walsh, C.A. (2003). Characterization of Foxp2 and Foxp1 mRNA and protein in the developing and mature brain. J. Comp. Neurol. *460*, 266–279.

Garel, S., and Rubenstein, J.L. (2004). Intermediate targets in formation of topographic projections: Inputs from the thalamocortical system. Trends Neurosci. *27*, 533–539.

Geisen, M.J., Di Meglio, T., Pasqualetti, M., Ducret, S., Brunet, J.F., Chedotal, A., and Rijli, F.M. (2008). Hox paralog group 2 genes control the migration of mouse pontine neurons through slit-robo signaling. PLoS Biol. *6*, e142.

Gomez, C., Ozbudak, E.M., Wunderlich, J., Baumann, D., Lewis, J., and Pourquie, O. (2008). Control of segment number in vertebrate embryos. Nature *454*, 335–339.

Grieshammer, U., Le, M., Plump, A.S., Wang, F., Tessier-Lavigne, M., and Martin, G.R. (2004). SLIT2-mediated ROBO2 signaling restricts kidney induction to a single site. Dev. Cell *6*, 709–717.

Hadjantonakis, A.K., Gertsenstein, M., Ikawa, M., Okabe, M., and Nagy, A. (1998). Generating green fluorescent mice by germline transmission of green fluorescent ES cells. Mech. Dev. *76*, 79–90.

Katz, M.J., Lasek, R.J., and Silver, J. (1983). Ontophyletics of the nervous system: Development of the corpus callosum and evolution of axon tracts. Proc. Natl. Acad. Sci. USA *80*, 5936–5940.

Kidd, T., Brose, K., Mitchell, K.J., Fetter, R.D., Tessier-Lavigne, M., Goodman, C.S., and Tear, G. (1998). Roundabout controls axon crossing of the CNS midline and defines a novel subfamily of evolutionarily conserved guidance receptors. Cell *92*, 205–215.

Kriegstein, A., Noctor, S., and Martinez-Cerdeno, V. (2006). Patterns of neural stem and progenitor cell division may underlie evolutionary cortical expansion. Nat. Rev. Neurosci. *7*, 883–890.

Leighton, P.A., Mitchell, K.J., Goodrich, L.V., Lu, X., Pinson, K., Scherz, P., Skarnes, W.C., and Tessier-Lavigne, M. (2001). Defining brain wiring patterns and mechanisms through gene trapping in mice. Nature *410*, 174–179.

Lin, J.C., Ho, W.H., Gurney, A., and Rosenthal, A. (2003). The netrin-G1 ligand NGL-1 promotes the outgrowth of thalamocortical axons. Nat. Neurosci. *6*, 1270–1276.

Long, H., Sabatier, C., Ma, L., Plump, A., Yuan, W., Ornitz, D.M., Tamada, A., Murakami, F., Goodman, C.S., and Tessier-Lavigne, M. (2004). Conserved roles for Slit and Robo proteins in midline commissural axon guidance. Neuron *42*, 213–223.

Lopez-Bendito, G., and Molnar, Z. (2003). Thalamocortical development: How are we going to get there? Nat. Rev. Neurosci. *4*, 276–289.

Lopez-Bendito, G., Cautinat, A., Sanchez, J.A., Bielle, F., Flames, N., Garratt, A.N., Talmage, D.A., Role, L.W., Charnay, P., Marin, O., and Garel, S. (2006). Tangential neuronal migration controls axon guidance: A role for neuregulin-1 in thalamocortical axon navigation. Cell *125*, 127–142.

Lopez-Bendito, G., Flames, N., Ma, L., Fouquet, C., Di Meglio, T., Chedotal, A., Tessier-Lavigne, M., and Marin, O. (2007). Robo1 and Robo2 cooperate to control the guidance of major axonal tracts in the mammalian forebrain. J. Neurosci. *27*, 3395–3407.

Ma, L., and Tessier-Lavigne, M. (2007). Dual branch-promoting and branch-repelling actions of Slit/Robo signaling on peripheral and central branches of developing sensory axons. J. Neurosci. *27*, 6843–6851.

Marillat, V., Cases, O., Nguyen-Ba-Charvet, K.T., Tessier-Lavigne, M., Sotelo, C., and Chedotal, A. (2002). Spatiotemporal expression patterns of slit and robo genes in the rat brain. J. Comp. Neurol. *442*, 130–155.

Marin, O., Plump, A.S., Flames, N., Sanchez-Camacho, C., Tessier-Lavigne, M., and Rubenstein, J.L. (2003). Directional guidance of interneuron migration to the cerebral cortex relies on subcortical Slit1/2-independent repulsion and cortical attraction. Development *130*, 1889–1901.

McManus, M.F., and Golden, J.A. (2005). Neuronal migration in developmental disorders. J. Child Neurol. *20*, 280–286.

Menuet, A., Alunni, A., Joly, J.S., Jeffery, W.R., and Rétaux, S. (2007). Expanded expression of Sonic Hedgehog in Astyanax cavefish: Multiple consequences on forebrain development and evolution. Development *134*, 845–855.

Metin, C., and Godement, P. (1996). The ganglionic eminence may be an intermediate target for corticofugal and thalamocortical axons. J. Neurosci. *16*, 3219–3235.

Metin, C., Alvarez, C., Moudoux, D., Vitalis, T., Pieau, C., and Molnar, Z. (2007). Conserved pattern of tangential neuronal migration during forebrain development. Development *134*, 2815–2827.

Mitrofanis, J., and Baker, G.E. (1993). Development of the thalamic reticular and perireticular nuclei in rats and their relationship to the course of growing corticofugal and corticopetal axons. J. Comp. Neurol. *338*, 575–587.

Molnar, Z., Adams, R., and Blakemore, C. (1998). Mechanisms underlying the early establishment of thalamocortical connections in the rat. J. Neurosci. *18*, 5723–5745.

Moreno, N., and González, A. (2007). Regionalization of the telencephalon in urodele amphibians and its bearing on the identification of the amygdaloid complex. Front Neuroanat. *1*, 1.

Moreno, N., González, A., and Rétaux, S. (2008). Evidences for tangential migrations in *Xenopus* telencephalon: Developmental patterns and cell tracking experiments. Dev. Neurobiol. *68*, 504–520.

Nagashima, H., Sugahara, F., Takechi, M., Ericsson, R., Kawashima-Ohya, Y., Narita, Y., and Kuratani, S. (2009). Evolution of the turtle body plan by the folding and creation of new muscle connections. Science *325*, 193–196.

Nguyen Ba-Charvet, K.T., Brose, K., Marillat, V., Kidd, T., Goodman, C.S., Tessier-Lavigne, M., Sotelo, C., and Chedotal, A. (1999). Slit2-Mediated chemorepulsion and collapse of developing forebrain axons. Neuron *22*, 463–473.

Nguyen-Ba-Charvet, K.T., Plump, A.S., Tessier-Lavigne, M., and Chedotal, A. (2002). Slit1 and slit2 proteins control the development of the lateral olfactory tract. J. Neurosci. *22*, 5473–5480.

Nguyen-Ba-Charvet, K.T., Picard-Riera, N., Tessier-Lavigne, M., Baron-Van Evercooren, A., Sotelo, C., and Chedotal, A. (2004). Multiple roles for slits in the control of cell migration in the rostral migratory stream. J. Neurosci. *24*, 1497–1506.

Niquille, M., Garel, S., Mann, F., Hornung, J.P., Otsmane, B., Chevalley, S., Parras, C., Guillemot, F., Gaspar, P., Yanagawa, Y., and Lebrand, C. (2009). Transient neuronal populations are required to guide callosal axons: A role for semaphorin 3C. PLoS Biol. *7*, e1000230.

Plump, A.S., Erskine, L., Sabatier, C., Brose, K., Epstein, C.J., Goodman, C.S., Mason, C.A., and Tessier-Lavigne, M. (2002). Slit1 and Slit2 cooperate to prevent premature midline crossing of retinal axons in the mouse visual system. Neuron *33*, 219–232.

Rajagopalan, S., Vivancos, V., Nicolas, E., and Dickson, B.J. (2000). Selecting a longitudinal pathway: Robo receptors specify the lateral position of axons in the *Drosophila* CNS. Cell *103*, 1033–1045.

Redies, C., Arndt, K., and Ast, M. (1997). Expression of the cell adhesion molecule axonin-1 in neuromeres of the chicken diencephalon. J. Comp. Neurol. *381*, 230–252.

Shu, T., Li, Y., Keller, A., and Richards, L.J. (2003a). The glial sling is a migratory population of developing neurons. Development *130*, 2929–2937.

Shu, T., Sundaresan, V., McCarthy, M.M., and Richards, L.J. (2003b). Slit2 guides both precrossing and postcrossing callosal axons at the midline in vivo. J. Neurosci. *23*, 8176–8184.

Simpson, J.H., Bland, K.S., Fetter, R.D., and Goodman, C.S. (2000). Short-range and long-range guidance by Slit and its Robo receptors: A combinatorial code of Robo receptors controls lateral position. Cell *103*, 1019–1032.

Simpson, T.I., Pratt, T., Mason, J.O., and Price, D.J. (2009). Normal ventral telencephalic expression of Pax6 is required for normal development of thalamocortical axons in embryonic mice. Neural Dev. *4*, 19.

Sylvester, J.B., Rich, C.A., Loh, Y.H., van Staaden, M.J., Fraser, G.J., and Streelman, J.T. (2010). Brain diversity evolves via differences in patterning. Proc. Natl. Acad. Sci. USA *107*, 9718–9723.

Tuorto, F., Alifragis, P., Failla, V., Parnavelas, J.G., and Gulisano, M. (2003). Tangential migration of cells from the basal to the dorsal telencephalic regions in the chick. Eur. J. Neurosci. *18*, 3388–3393.

Uemura, M., Nakao, S., Suzuki, S.T., Takeichi, M., and Hirano, S. (2007). OL-Protocadherin is essential for growth of striatal axons and thalamocortical projections. Nat. Neurosci. *10*, 1151–1159.

Verney, C., Zecevic, N., and Ezan, P. (2001). Expression of calbindin D28K in the dopaminergic mesotelencephalic system in embryonic and fetal human brain. J. Comp. Neurol. *429*, 45–58.

Wu, W., Wong, K., Chen, J., Jiang, Z., Dupuis, S., Wu, J.Y., and Rao, Y. (1999). Directional guidance of neuronal migration in the olfactory system by the protein Slit. Nature *400*, 331–336.

Zhou, L., Bar, I., Achouri, Y., Campbell, K., De Backer, O., Hebert, J.M., Jones, K., Kessaris, N., de Rouvroit, C.L., O'Leary, D., et al. (2008). Early forebrain wiring: Genetic dissection using conditional Celsr3 mutant mice. Science *320*, 946–949.

Zhu, Y., Li, H., Zhou, L., Wu, J.Y., and Rao, Y. (1999). Cellular and molecular guidance of GABAergic neuronal migration from an extracortical origin to the neocortex. Neuron *23*, 473–485.